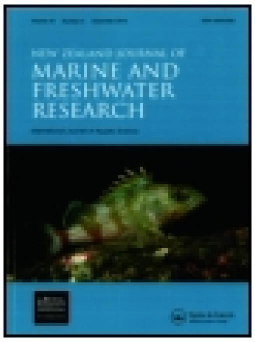

New Zealand Journal of Marine and Freshwater Research

ISSN: 0028-8330 (Print) 1175-8805 (Online) Journal homepage: http://www.tandfonline.com/loi/tnzm20

Short period (1–4 h) sea level fluctuations on the Canterbury coast, New Zealand

Derek G. Goring & R. Falconer Henry

To cite this article: Derek G. Goring & R. Falconer Henry (1998) Short period (1–4 h) sea level fluctuations on the Canterbury coast, New Zealand, New Zealand Journal of Marine and Freshwater Research, 32:1, 119-134, DOI: 10.1080/00288330.1998.9516811

To link to this article: http://dx.doi.org/10.1080/00288330.1998.9516811

New Zealand Journal of Marine and Freshwater Research, 1998, Vol. 32: 119–134

0028–8330/98/3201–0119 $7.00/0

Short period (1–4 h) sea level fluctuations on the Canterbury coast, New Zealand

DEREK G. GORING
National Institute of Water & Atmospheric Research Ltd
P. O. Box 8602
Christchurch, New Zealand

R. FALCONER HENRY
Triton Consultants Ltd
3530 W. 43rd Avenue
Vancouver, B.C., Canada

Abstract Data from six sea level sites on the Canterbury coast, New Zealand, were analysed for short period (1–4 h) waves. Persistent waves with periods of 3.4 h in Pegasus Bay and 2.4 h in the Canterbury Bight were found. Their amplitude and phase are highly variable. Edge waves of similar period were found in simulations using a 2-dimensional, harmonic, shallow water, numerical model. Numerical and analytical modelling showed that the offshore decay in amplitude may be approximated by Stokes zero-mode edge waves, but the numerical model revealed that the detailed structure of the offshore decay is more complicated than can be explained by analytical models using a semi-infinite sloping beach. Rotation appears to have little effect. In Pegasus Bay the edge waves are trapped laterally between the northern extent of the bay and Banks Peninsula and offshore by the shelf. In the Canterbury Bight they are trapped laterally between Banks Peninsula and the curvature of the coast and offshore by the shelf. The origin of the waves and the reason for their variability are unclear, but may be the result of the non-linear interaction between semidiurnal tides and meteorological effects.

Keywords water waves; edge waves; coastal trapped waves; seiche; Canterbury

---

M97033
Received 11 July; accepted 16 September 1997

INTRODUCTION

Some sea level records on the eastern coast of the South Island of New Zealand (Fig. 1) exhibit significant distortion on the peaks and troughs of the signal (Fig. 2A). The cause of this distortion is waves of periods between 2 and 4 h (Fig. 2B, C). These waves are a persistent feature of the sea level records from all locations along the Canterbury coast. Heath (1979, 1982) found such waves, but only at 2.5 h period, whereas, our analysis of any period of record from the new, open-coast recorder at Sumner Head (established June 1994) indicates that their period is predominantly 3.4 h. The origin of the waves is unlikely to be purely tidal (although their period corresponds to an S_7 tide) because at a particular location their amplitude and phase vary with time; whereas, we would expect that compound-tides or overtides caused by non-linear interaction between tidal constituents as the tide propagates into shallow water would have constant amplitude and phase at a particular location. Furthermore, there appears to be no simple correlation between the amplitude of the waves and weather events (either local or global winds, or barometric pressure fluctuations).

Heath (1982) used the linearised, 2-dimensional, shallow water equations to determine the modal structure of 2.5 h edge waves on the east coast of New Zealand. Using the bathymetry in lines normal to the coastline, he showed that for 2.5 h edge waves, alongshore wavelengths on the east coast continental shelf are typically c. 1465 km and for the Chatham Rise c. 1340 km. He hypothesised that the alongshore waves on the east coast have antinodes at Banks Peninsula and Hawke Bay and the alongshore waves on the Chatham Rise have an antinode at the coast and a node east of the Chatham Islands. As supporting evidence he used data from tide gauges at Lyttelton, Timaru, Wellington and the Chatham Islands as well as response to the 1960 Chilean and 1964 Alaskan tsunamis. The data indicate maxima at Lyttelton and Timaru and minima at Wellington which is consistent with the alongshore waves on the east

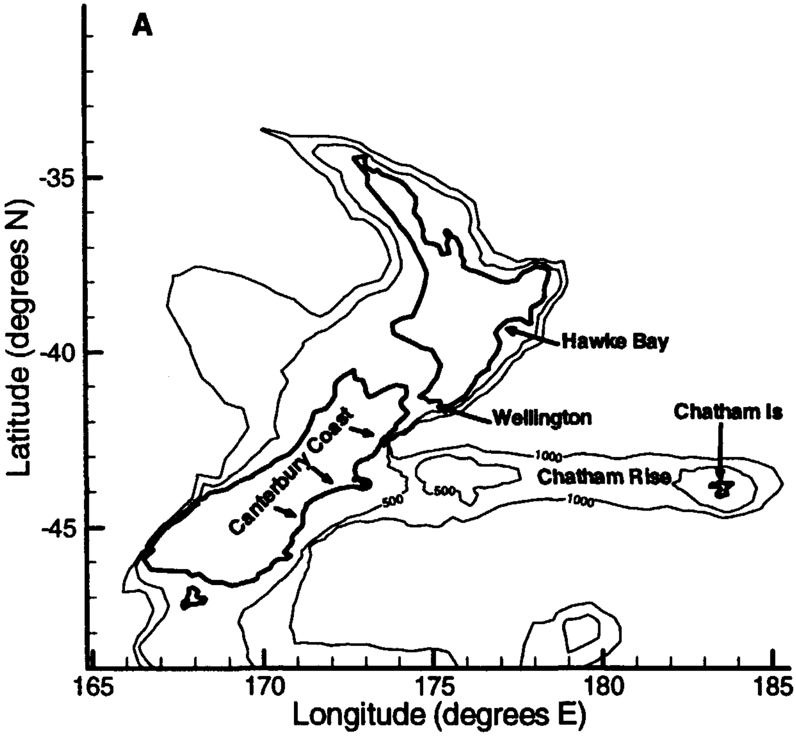

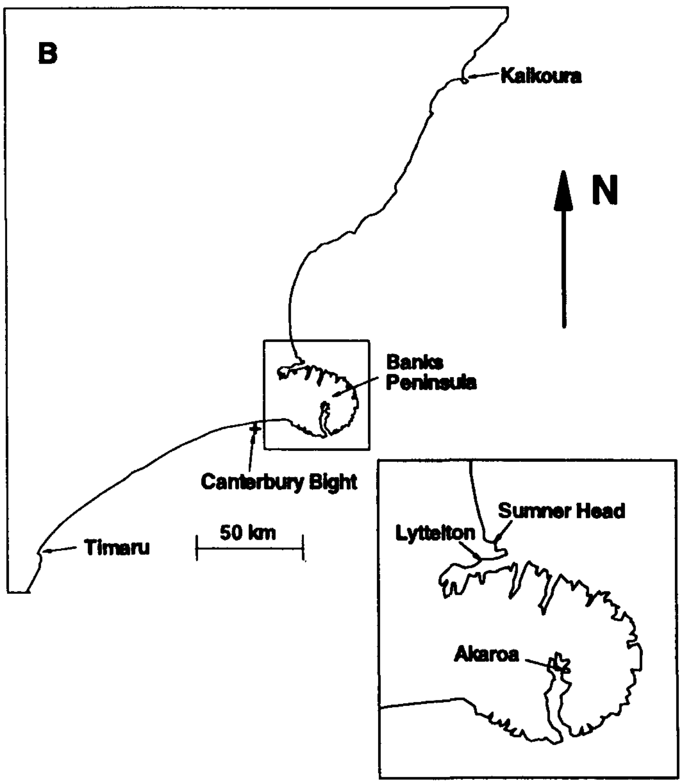

Fig. 1 **A,** New Zealand region showing the 500 and 1000 m contours and the area under consideration; and **B**, detailed plots of the Canterbury coast showing the locations of sea level recording sites.

Fig. 2 Typical piece of record from Sumner Head, New Zealand, showing: **A**, 2 days of raw data; **B**, the short period (1–4 h) fluctuations; and **C**, the power spectral density function.

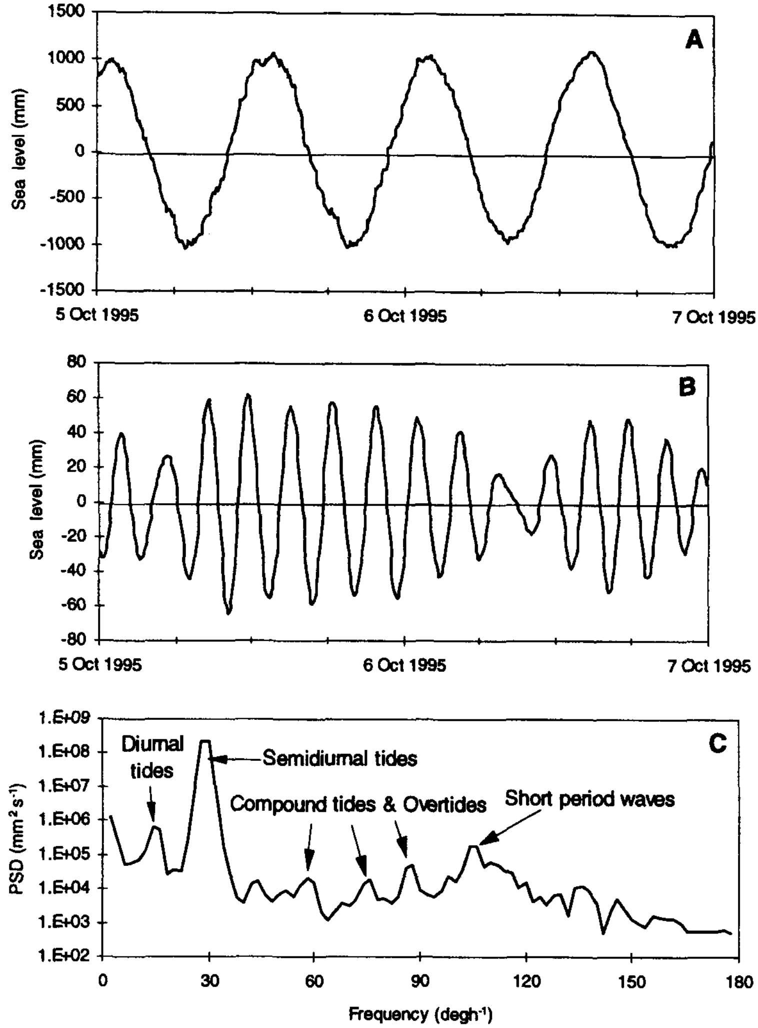

coast having antinodes at Banks Peninsula and Hawke Bay and a node at Wellington. The absence of a 2.5 h signature at the Chatham Islands is consistent with the wave along the Chatham Rise having a node just east of the Chatham Islands. However, Heath also noted that data from a recorder installed at Kaikoura showed no 2.5 h signature. He concluded that some excitation other than standing waves on the east coast continental shelf and the north slope of the Chatham Rise was involved. This inconsistency, the spasmodic nature of the 2.5 h oscillations and the presence of persistent 3.4 h oscillations, not reported by Heath, led to the detailed investigation reported here.

The bathymetry off the Canterbury coast is irregular (see Fig. 1). At Kaikoura, in the north, the 500 m depth contour is within a few km of the shoreline, yet at Banks Peninsula, only 150 km to the south, the 500 m depth contour extends 1000 km to the east beyond the Chatham Islands. South of Banks Peninsula, the bathymetry is gently sloping, with the 500 m contour c. 100 km offshore.

The Chatham Rise is the major feature of this bathymetry and is widely believed to have a dominant effect on coastal sea levels on the Canterbury coast (Heath 1982). Work on currents in the vicinity of the Chatham Rise by Heath (1983), Greig & Gilmour (1992), and Chiswell (1994) indicate that they are dominated by the M_2 tide with smaller diurnal tides also present. None of these studies report evidence of oscillations at the shorter periods under consideration here.

This paper reports the results of analysis of the observations of short period waves at six locations along the Canterbury coast. Unfortunately, the records at these sea level stations are not all coincident. Thus, the spatial distribution of the waves cannot be easily determined from the historical data. In an effort to explain the presence of these waves, analytical and numerical models were considered.

OBSERVATIONS AND METHODS

Data analysis

Sea level data

Sea level data are available from six sites on the Canterbury coast as indicated in Table 1. The Akaroa and Canterbury Bight records are from short-term deployments of bottom-mounted tide gauges. The remaining records are from permanent, shore-mounted sea-level recorders, however the Timaru record is of poor quality and the data availability is patchy. Only the Kaikoura, Canterbury Bight, and Sumner Head records are from open-coast sites, the remainder are in harbours and thus may contain locally-generated oscillations. The data were sampled at 5 min intervals, except for Canterbury Bight for which the data were sampled at 15 min intervals.

For the analysis, the short Akaroa and Canterbury Bight records were used in their entirety, but for the remaining sites 229 days of coincident data (from 6 August 1995 to 23 March 1996) were analysed.

Band-pass filtering

Since the primary focus of this study was on the short period waves (1–4 h), the records were band-pass filtered to remove all but these waves. The filter chosen was a tapered boxcar filter in the frequency domain (see Goring & Bell 1996). For this filter the data are transformed to the frequency domain, then a boxcar transfer function with ends tapered by tanh functions is applied and the data are transformed back to the time domain. Advantages of this filter are that the tide is removed completely (i.e., there is no possibility of leakage of semidiurnal tides into higher frequencies), there is no attenuation of the data in the band under consideration and the phase is unchanged.

Spectral analysis

Two forms of spectral analysis were carried out—Fourier and Pisarenko. Standard techniques were used for Fourier analysis (see e.g., Otnes & Enochson 1978) using the FFT (Fast Fourier Transform). Fourier analysis requires an assumption of linearity in the signal. There is no recognition that observed energy at one frequency could have been generated by non-linear interactions of energies at other frequencies. For example, the compound MS_4 tide formed by non-linear interaction of the M_2 and S_2 tides appears as an identifiable spike in the Fourier spectrum, yet it only arises because of the interaction of the two semidiurnal tides. Therefore, for the analysis of short period waves such as are shown in Fig. 2, we need to determine to what extent these waves arise because of the non-linear interaction of energy from other parts of the spectrum (Marone & de Mesquita 1994). The Pisarenko spectrum and the bispectral density function which arises from it allow for this because noise arising from linear systems do not appear in the bispectrum (Bendat 1990). Therefore, any energy appearing in the bispectrum at frequencies other than the forcing frequencies must

Table 1 Sea level data used in the analysis. (Agencies are: NIWA, National Institute of Water and Atmospheric Research Ltd; UC, University of Canterbury; CRC, Canterbury Regional Council; LPC, Lyttelton Port Co.; and TPC, Timaru Port Co.)

		Data availability		
Site	Agency	Start	Finish	Comments
Kaikoura	NIWA/UC	940831	Present	No gaps
Sumner Head	NIWA/CRC	940604	Present	Gap 941004–941120
Lyttelton	LPC	940601	960412	No gaps
Akaroa	NIWA	910323	910513	No gaps
Canterbury Bight	NIWA	840628	840726	No gaps, 15 min data
Timaru	TPC	940601	960323	Many gaps and errors

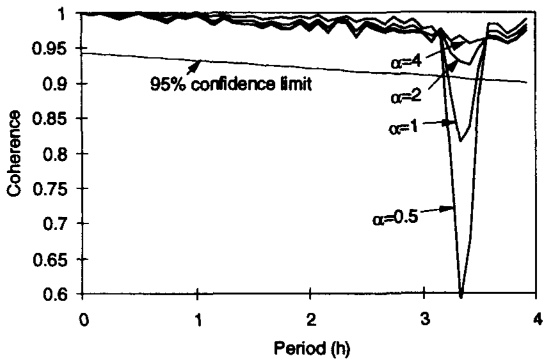

Fig. 3 Results of phase coherence analysis on the noisy signal (Equation 5) for various levels of noise.

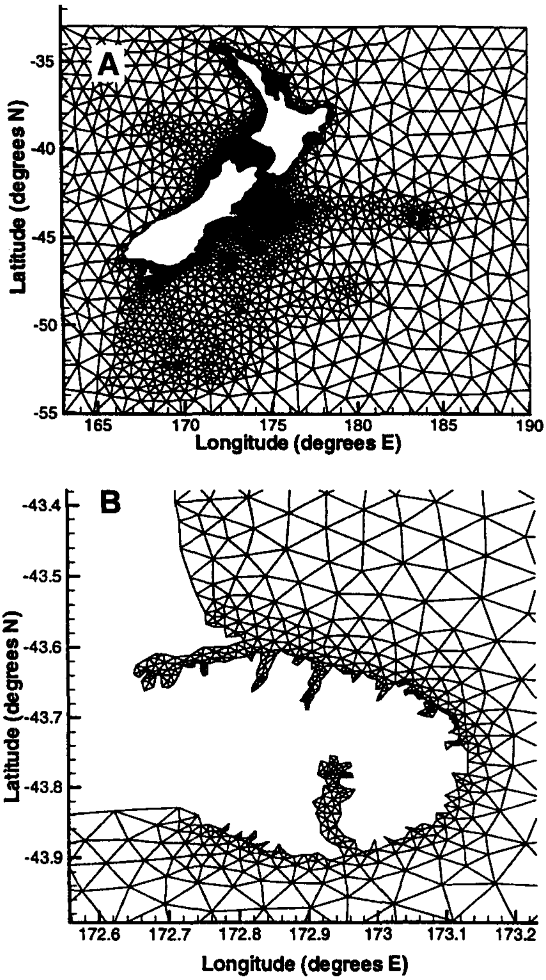

Fig. 4 Finite element grid: **A**, for entire domain; and **B**, detailed grid in the vicinity of Banks Peninsula, New Zealand.

arise from a non-linear process. Thus, the Pisarenko spectrum and bispectrum (Pisarenko 1972) have been used to detect the origin of non-linearities in tidal signals by Marone & de Mesquita (1994). Unfortunately, the latter paper contains some serious typographical errors in the mathematical equations which may have prevented the method being applied widely. The correct equation for the Pisarenko spectral estimate $h(f_j)$, is:

$$h(f_j) = \frac{1}{2n} A_{jk} \lambda_k \tag{1}$$

where $f_j = (j-1)/(n\Delta t)$, $j = 1,2,...n$ is the frequency, λ_k are the eigenvalues of the autocovariance matrix formed by grouping the N data at time intervals of Δt into m sets of n data each, and repeated indices indicate summation. The matrix A is formed by combining the matrix of eigenvectors, a_{jk}, and a matrix of exponentials as follows:

$$A_{jk} = \left| a_{jk} \exp\{i(k-1)\pi f_j\} \right|^2 \tag{2}$$

where $i = \sqrt{-1}$. The bispectral density function is:

$$H(f_j f_k) = A_{jl} A_{kl} \lambda_l \tag{3}$$

Determining periodicity

There are numerous methods available for determining periodicity in a signal. Fourier analysis can be used, but the precision depends upon the length of record used, viz., the frequency interval $\Delta f = 1/N\Delta t$, where N is the number of data and Δt is the data interval. Thus, for example, for 2-day samples consisting of 48-hourly data, $\Delta f = 7.5°/h$, which for periods in the vicinity of 3.4 h corresponds to a precision of c. 0.25 h. Another alternative is autocorrelation which has the advantage of higher precision (i.e., the data interval, which was 5 min for most of the data). However, the periodogram produced tends to be too smooth to identify periods which are close together. Therefore, periodicity was determined using the phase coherence method of Lindstrom et al. (1997). This method calculates the phase coherence function by the following steps: (1) split the data sequence $y(i)$, $i = 1, N$ into k subsets:

$$\begin{aligned} S_1 &= \{y(1), y(k+1), y(2k+1, ...\} \\ S_2 &= \{y(2), y(k+2), y(2k+2, ...\} \\ &\dots \\ S_k &= \{y(k), y(2k), y(3k), ...\} \end{aligned} \tag{4}$$

(2) remove the mean from each of these subsets; (3) reassemble the subsets into a single data

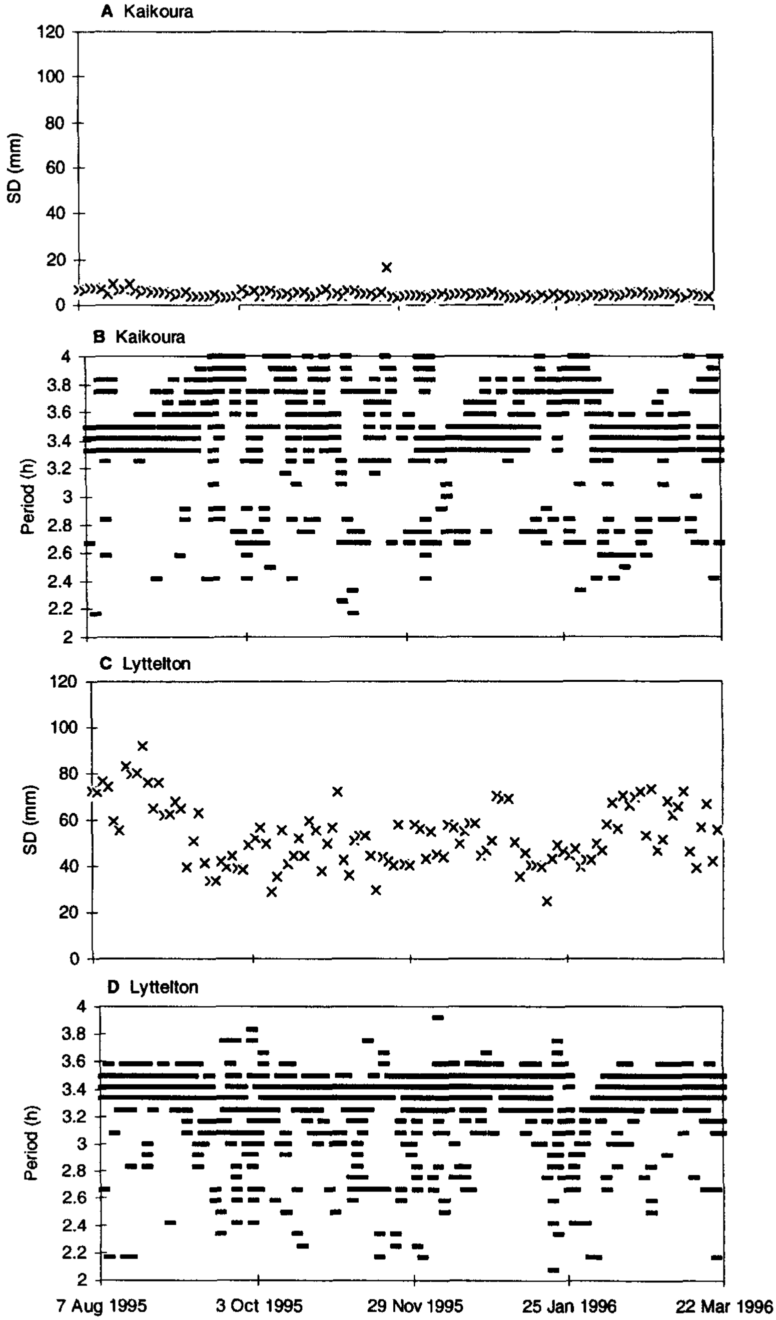

Fig. 5 Standard deviation (SD) and periodicity of 2-day samples from concurrent records from: **A** and **B**, Kaikoura; **C** and **D**, Lyttelton; **E** and **F**, Sumner Head; and **G** and **H** Timaru, New Zealand.

sequence; and (4) calculate the standard deviation C_k of the reassembled data.

The sequence C_k for $k = 1, N$ is the phase coherence function. Downward spikes of C_k below a threshold, representing a local minimum of variance, indicate periodicity at that value of k.

Numerical experiments were carried out to assess how well this method can detect periodicity in a noisy signal such as:

$$y(t) = \cos(2\pi t/T) + \alpha\varepsilon(t) \quad (5)$$

where T is the period, ε is white noise (Gaussian distributed random numbers with zero mean and

Fig. 5 (*continued*)

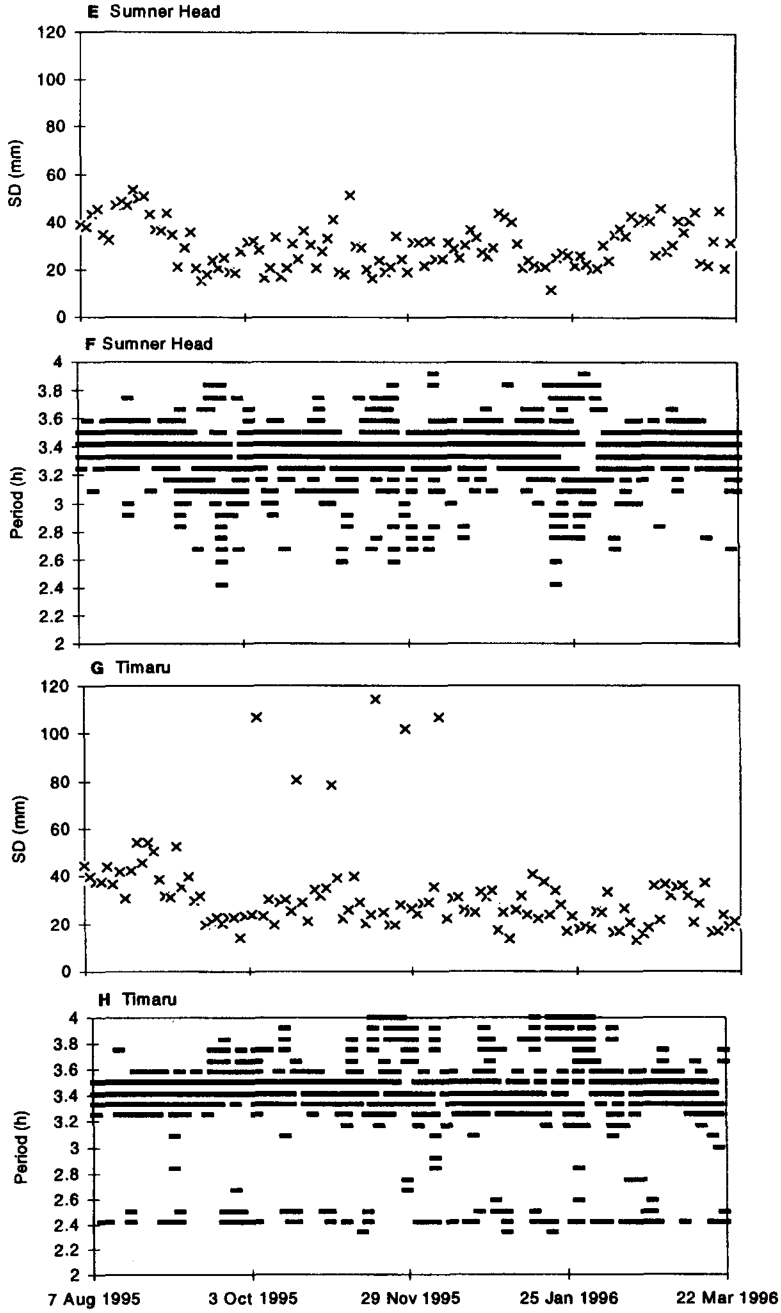

unit standard deviation), and α is the proportion of noise to signal. The results, for $T = 3.4$ h and various α, are presented in Fig. 3 and show that providing the noise is of the same order as the periodic part of the signal or less, phase coherence analysis will detect the periodicity. However, the method has trouble detecting periodicity if the standard deviation of the noise is greater than twice the amplitude of the signal.

We extended the method of Lindstrom et al. (1997) by normalising the phase coherence, C_k, with respect to the standard deviation of the total series, C_1, and defining a binary function:

$$C'_k = 0 \text{ for } C_k \geq L_k \text{ and}$$
$$C'_k = 1 \text{ for } C_k < L_k \qquad (6)$$

where L_k is the 95% confidence limit. By applying the analysis to a moving window of data, a time sequence of periodicity is generated which shows how waves of various periods wax and wane with time.

Models

Analytical models

LeBlond & Mysak (1978) give a summary of the analytical models available for coastal trapped waves or edge waves arising from the solution of the linearised shallow water equations for simplified geometries. The general form of the solutions is:

$$\eta = F(x)\exp\{i(ky-\omega t)\} \qquad (7)$$

where η is amplitude of the water surface, k is wave number, ω is radial frequency, x is distance from shore, y is distance along the coastline, and t is time. Depending upon the assumptions made, the function $F(x)$ and the dispersion relation (the relationship between frequency and wave number) take different forms. The classical solution of Stokes, arrived at by assuming irrotational flow (no Coriolis force) is:

$$F(x) = A_0\exp\{-(k\cos\beta)x\} \qquad (8)$$

with dispersion relation:

$$\omega^2 = gk\sin\beta \qquad (9)$$

where A_0 is a constant, β is the slope of a semi-infinite beach, and g is the acceleration of gravity. By including the effect of rotation, LeBlond & Mysak (1978) give the Reid solution:

$$F_n(x) = A_n \exp\{-kx\}L_n(2kx)$$
$$\omega_n^3 - \{f^2 + (2n+1)gk\tan\beta\}\omega_n - fgk\tan\beta = 0 \qquad (10)$$

where n is the mode of the solution ($n = 0,1,2,.....$), f is the Coriolis force, and L_n is the nth degree Laguerre polynomial. In the Southern Hemisphere (where f is negative) the dispersion relation has two positive roots and one negative root. The negative root represents a first-class edge wave which propagates with the coastline on its left. One of the positive roots is also a first-class edge wave which propagates with the coastline on its right and the third root is a second-class edge wave with an extremely large wave length which LeBlond & Mysak call a quasi-geostrophic wave. The Reid solution collapses to the Stokes edge wave for $f = 0$, $n = 0$, and $\cos\beta = 1$.

Numerical model

The analytical models of Stokes and Reid assume a simplified geometry of an infinite straight coastline and a semi-infinite beach of constant slope. In reality, on the Canterbury coast, these assumptions are a gross simplification, as shown in Fig. 1. Therefore, numerical modelling was undertaken to more adequately account for the bathymetry and the curvature of the coast. The numerical model chosen was TIDE2D, the 2-dimensional, frequency domain, finite element model of Walters (1988). The model solves the depth-averaged Navier-Stokes equations with a free surface. A frequency domain model was used in preference to a time-stepping model because of the strongly periodic nature of the short period waves. Thus, we were able to excite the model at a range of frequencies in turn and measure the response. Non-linear responses could be detected by exciting the model at one frequency and calculating the response of higher harmonics. To excite the model we used low level winds from various directions over the whole domain. Because of the size of the domain being modelled (33–55°S and 163–190°E), spherical polar coordinates were used for the coordinate system, thus allowing for the curvature of the earth in the calculations. The following parameters were used in the model: (1) Coriolis parameter was evaluated at 44°S and assumed to be constant over the grid; (2) quadratic friction in the form:

$$\tau_b = C_f \frac{\vec{u}\,|\vec{u}\,|}{gh} \qquad (11)$$

was assumed, where τ_b is the bottom shear stress, $\vec{u}$ is the velocity vector, and C_f is the friction coefficient assumed to be $C_f = 0.00025$.

Gridding algorithm

The TRIGRID method of Henry & Walters (1993) was used to produce a finite element grid of the New Zealand region (Fig. 4). The algorithm produces triangular elements of approximately equilateral shape whose area is proportional to the depth. Thus, for long waves which travel at speeds of approximately $\sqrt{gh}$, where g is the acceleration of gravity and h is the depth, waves in shallow water near the coast take the same time to cross an element as those in the deep ocean. This property is important in ensuring the

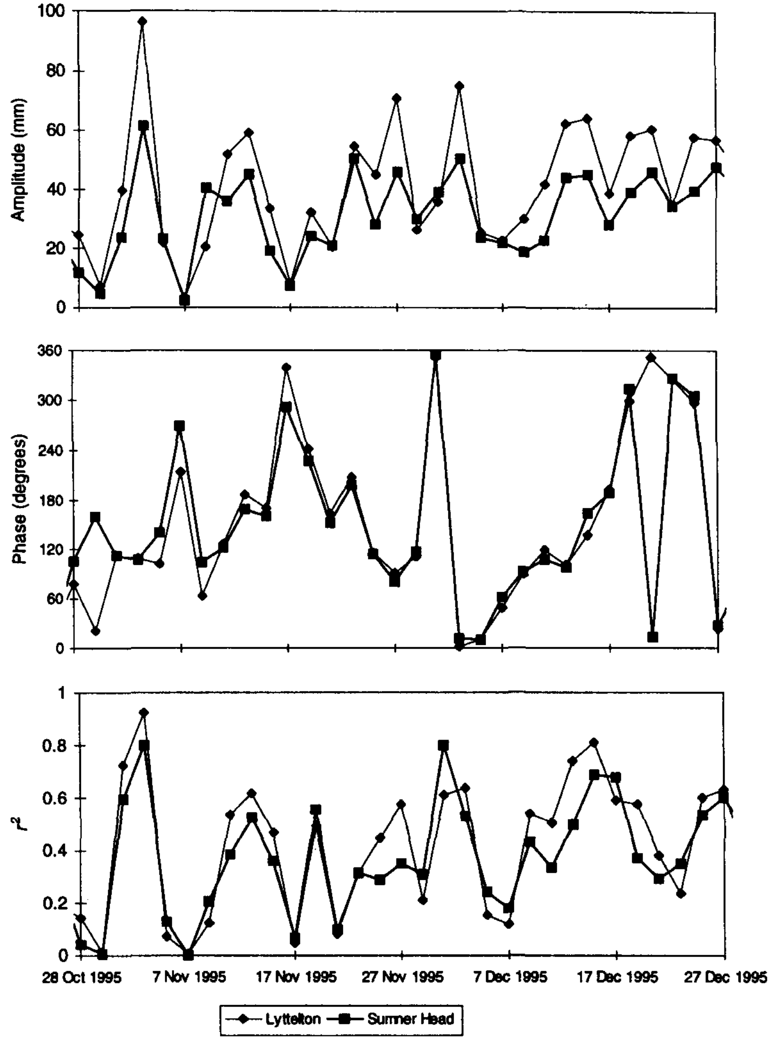

Fig. 6 Results of fitting a sine wave with period 3.4 h to data from Lyttelton and Sumner Head, New Zealand.

stability of any numerical scheme which uses such a grid.

Figure 4 shows the two aspects of the finite element mesh—a coarse grid of the wider New Zealand ocean region (using GEBCO bathymetry data) and a fine grid of the ocean in the vicinity of the Canterbury coast (using bathymetry data digitised from charts by Herzer (1977a,b; 1980) and Herzer & Carter (1983)). The fine grid is nested within the coarse grid, with elements as small as 230 m on a side close to the coast and as large as 230 km on a side in deep water. This technique of progressive refinement of the grid as the coast is approached has been demonstrated to yield highly accurate solutions for propagation of tides (Davies et al. 1997).

RESULTS

Sea level data analysis

Phase coherence analysis

Results of the phase coherence analysis for periodicity of Lindstrom et al. (1997), extended to accommodate a moving window and normalisation, are presented in Fig. 5 for the four sea level sites with concurrent records. Each site has two plots—standard deviation, which is a measure of the overall

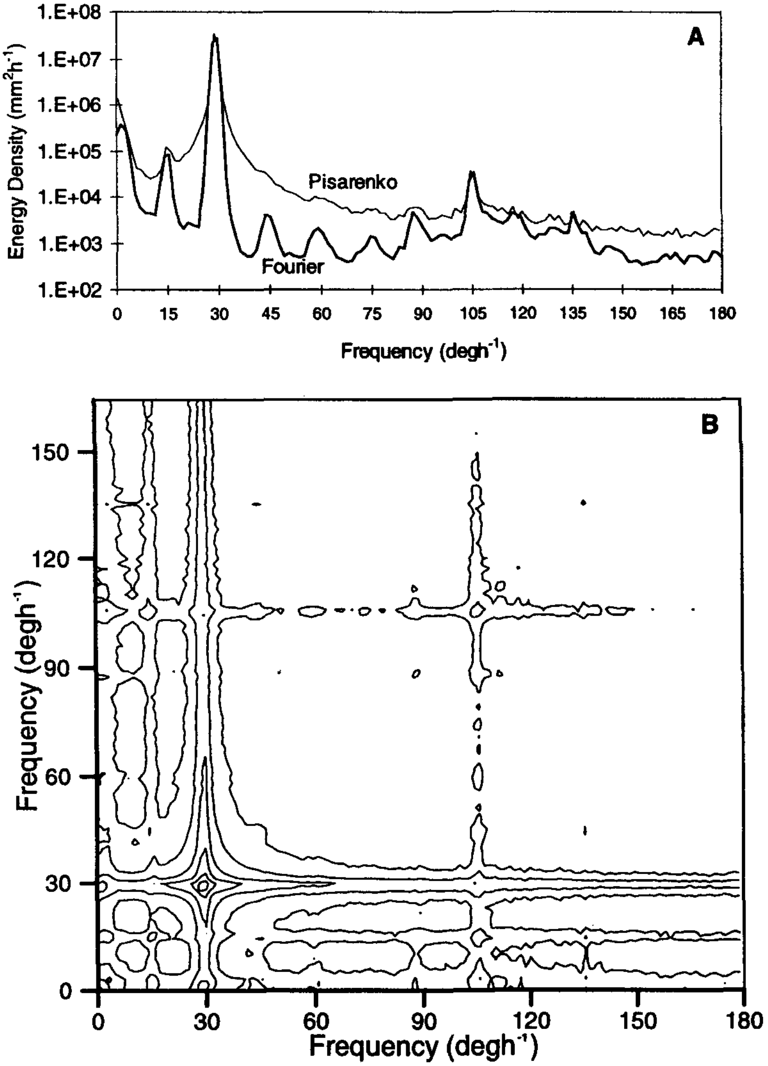

Fig. 7 Spectral analysis for 228 days of Sumner Head, New Zealand data showing: **A**, Fourier (solid line) and Pisarenko (thin line) spectra; and **B**, the bispectrum with contours at intervals of 10^n, n = 2, 3 , ...7. The sequence was split into 21 sets of 256 data at hourly intervals.

strength of the signal, and periodicity. Each point on the graphs represents the standard deviation and periodicity of a 2-day sample. Periodicity is represented by a horizontal bar if the binary phase coherence function, C'_k from Equation 6 is unity and a blank if it is zero. Thus, continuous lines on the periodicity plots represent persistent energy at that period, whereas patchy lines represent spasmodic energy at that period. The plots show that waves with period 3.4 h occur almost always at all four sites. However, at Kaikoura, where the standard deviation of the signal is usually an order of magnitude less than elsewhere, the waves tend to be the most spasmodic, with waves of many other periods also present. The periodicity data from Sumner Head and Lyttelton appear to be essentially the same. In fact, the standard deviation at Lyttelton on average is 149% greater than that at Sumner Head with a coefficient of determination r^2 = 0.886, indicating that these are usually the same waves which are amplified as they propagate into the harbour. Visual inspection of the standard deviations in Fig. 5C (Lyttelton) and Fig. 5F (Timaru) appears to show some similarity between the records. However, this is not the situation, because the correlation is low (r^2 = 0.014), even excluding the six outliers in the Timaru record.

Of the other two records, Akaroa exhibits a similar pattern to Timaru, but also shows some

Fig. 8 Sea level responses to: **A** and **B**, north winds; and **C** and **D**, east winds at locations north of Banks Peninsula (A and C) and south of Banks Peninsula, New Zealand (B and D).

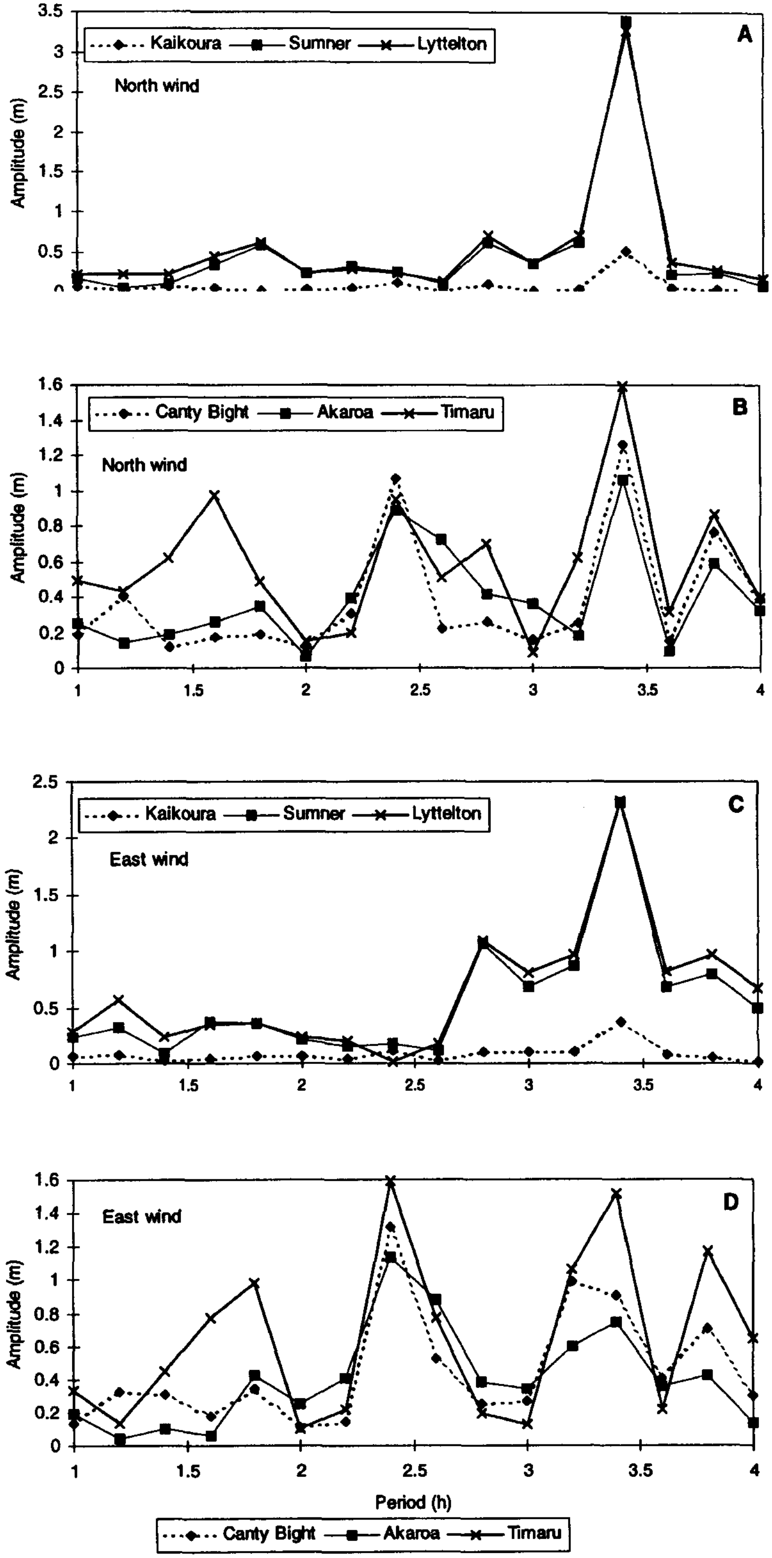

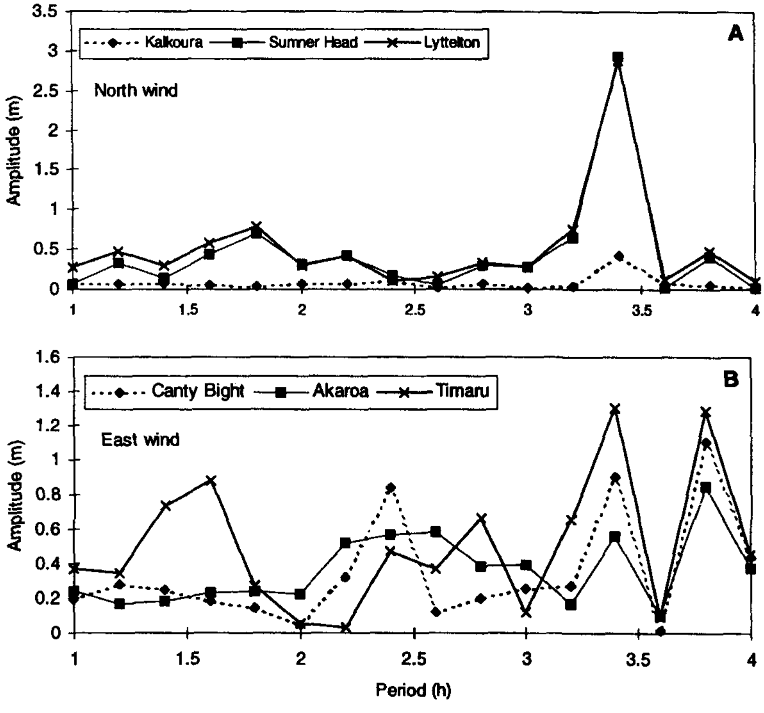

Fig. 9 Sea level responses (in the absence of Coriolis force) to north winds at locations: **A**, north of Banks Peninsula; and **B**, south of Banks Peninsula, New Zealand.

periodicity at 2 h. The Canterbury Bight record shows periodicity at 2.4 h and from 3.4 to 4 h, however, the short record (26 days) is insufficient to detect the overall pattern very clearly.

All records show significant variability in standard deviation as a function of time indicating the high degree of non-stationarity of this frequency band.

Analysis with a moving spectral window

The results of fitting a 3.4 h period sine wave to data from Sumner Head and Lyttelton are presented in Fig. 6. The amplitudes of the waves at Lyttelton are generally greater than those at Sumner Head, as noted earlier when considering the overall strength of the signal. However, the phases are equal most of the time, indicating that these are the same waves. Both amplitude and phase vary considerably with time and there is no apparent pattern to the variation. The coefficient of determination, r^2, which represents the proportion of the energy at 3.4 h period which can be attributed to a sine wave at that period, also exhibits considerable variability with time, but there is similarity between Sumner Head and Lyttelton. When the amplitude of the waves is small, r^2 is also small and there is often a significant difference between the phases for the two sites.

Spectra and bispectra

The results of spectral analysis are presented in Fig. 7, showing that the Pisarenko and Fourier spectra give the same results for most of the range of frequencies, except for the compound and overtides in the vicinity of 45, 60, and 75° h^{-1} which do not appear in the Pisarenko spectrum. The bispectrum shows cells of energy over the whole frequency range at 105° h^{-1} (3.4 h period), indicating that these waves are related in some way to the diurnal and semidiurnal tides, as well as the low frequency weather band. This suggests that a likely source of the short period waves under consideration is non-linear interaction between tides and meteorological effects.

Model results

A series of model runs was carried out using the model grid shown in Fig. 4 and using low-level winds from the north and from the east at periods from 1 to 4 h in steps of 0.2 h to excite the water surface. For each run, corresponding to a particular period and wind direction, the model produced

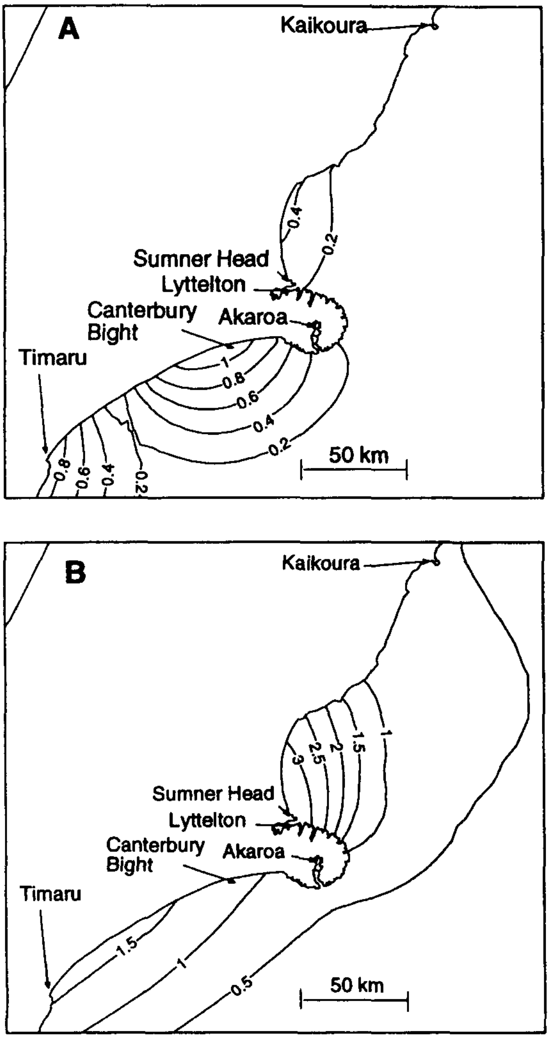

Fig. 10 Spatial distribution of sea level response at: **A**, 2.4 h period; and **B**, 3.4 h period.

responses at each node for the three variables (sea level and two horizontal velocities) in the form of complex numbers which could be converted to the amplitude and phase for that variable for that period.

Sea level responses at the nodes corresponding to the various recording sites (Fig. 1 and Table 1) for the range of periods from 1 to 4 h and for the two wind directions (east and north) are presented in Fig. 8. The figure shows that the 3.4 h periodicity observed in the data is also replicated in the model for all sites and that there is also periodicity at 2.4 h periods for sites south of Banks Peninsula. The modelled response at Lyttelton was generally larger than that at Sumner Head, which was also observed in the data. As a test of the effect of the earth's rotation on these results, the model runs using a north wind were repeated with the Coriolis force turned off (Fig. 9). Fig. 9A should be compared with Fig. 8A and Fig. 9B should be compared with Fig. 8B. The data indicate that the effect of rotation is to generally amplify the response, but the periodicities are not changed.

The spatial distribution of the 2.4 and 3.4 h period waves are presented in Fig. 10 and Fig. 11. The results shown there are for forcing by north/south winds, but forcing in other directions produces almost identical results. The 2.4 h period waves (Fig. 10A) exhibit two classical edge wave cells in the Canterbury Bight and the 3.4 h period waves (Fig. 10B) have a cell in Pegasus Bay. In both instances the cells have a focal point at the point of largest curvature of the coastline. In Fig. 11 the profiles through the centres of the edge wave cells are compared with the analytical models of Stokes and Reid for straight coastline and semi-infinite slope. In the calculations, the slope for Pegasus Bay was 0.083°, representing the 71 m increase in depth over 49 km from shore to the shelf edge and for the Canterbury Bight the slope was 0.103°, representing the 130 m increase in depth over 73 km from shore to the shelf edge.

DISCUSSION

The work of Heath (1982) can now be re-assessed in the light of better quality sea level data and with more sophisticated models than were available in the early 1980s. Heath used a one-dimensional model which assumed an infinite coastline and a semi-infinite sloping beach, whereas our model is able to accommodate the highly variable 3-dimensional shape of the coastline and bathymetry (Fig. 1). Thus, our results show that Heath's hypothesis that the 2.5 h edge waves extend from Canterbury to Hawke Bay is false. In fact, both the data and our numerical modelling have shown that the edge waves have two predominant periods: 3.4 h in Pegasus Bay and 2.4 h in the Canterbury Bight. Furthermore, our numerical modelling shows that the edge waves in the Canterbury Bight are confined laterally by Banks Peninsula and the Chatham Rise to the north and have a node just north of Timaru to the south. The edge waves in Pegasus Bay are confined between Banks Peninsula and the Chatham Rise and the northern end of Pegasus Bay. The

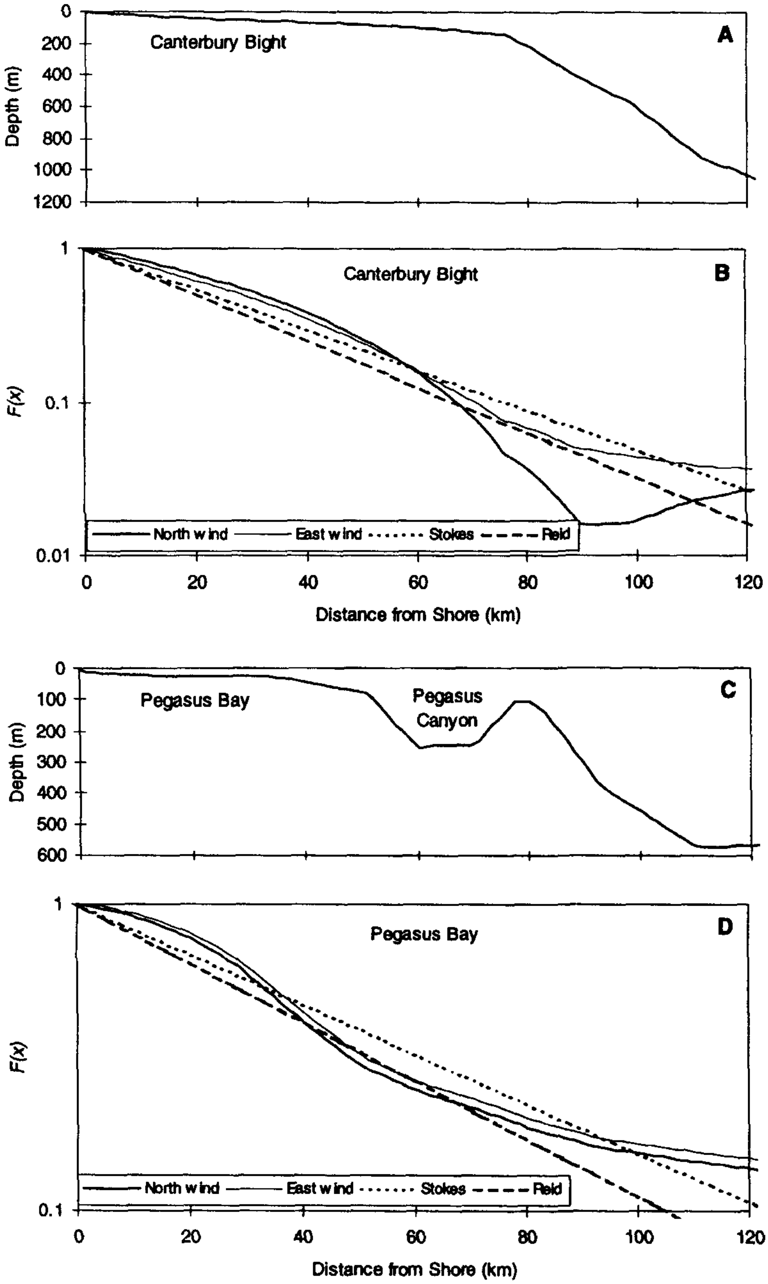

Fig. 11 Sections through: (**A** and **B**) Canterbury Bight for 2.4 h period waves and (**C** and **D**) Pegasus Bay, New Zealand for 3.4 h period waves.

reason that Heath's hypothesis is false is that it was based on the oversimplified assumption that the coastline is infinite and straight, which it is not. Our findings indicate that this assumption is important in determining the alongshore shape of the edge waves. On the other hand, when we consider the shape of the function $F(x)$ of Equation 7 defining how the waves decay in amplitude in an offshore direction, we find that the assumption of a semi-infinite sloping beach is not such a serious simplification in terms of the overall rate of decay. This is illustrated in Fig. 11 which shows that the rate of decay of amplitude predicted to be exponential by the analytical models of a semi-infinite sloping beach is roughly the same as the shape of the function from the numerical model. The figure also shows that the Reid model, which accounts for rotation and gives a slower rate of decay than the Stokes model, is a closer approximation to the numerical model. Nevertheless, the detailed shape of $F(x)$ from the numerical model is not exponential, but has a convex shape near the coast and for Pegasus Bay (Fig. 11D) only becomes concave at a distance of between 30 and 40 km from shore. LeBlond & Mysak (1978) describe an analytical model for determining edge waves on a sloping shelf of finite width in terms of Laguerre polynomials, $L_v(2kx)$, where v is a non-integer value derived from the dispersion relation. Unfortunately, non-integer Laguerre polynomials are difficult to calculate ($L_v(z) \equiv M(-v;1;z)$, where M is the confluent hypergeometric function), but inspection of numerical tables in Abramowitz & Stegun (1964) indicates that for small z, the shape of $L_v(z)$ for all v is concave, therefore, we postulate that the finite width of the shelf is not the cause of the convex shape of $F(x)$ in the numerical model. Whether this shape can be explained analytically remains uncertain. However, we suggest that the problem could be simplified by neglecting rotation, since we have found that its inclusion makes almost no difference to the numerical results.

Upon the matter of what generates the edge waves and why their amplitude and phase are so variable, the bispectrum (Fig. 7B) indicates that energy from the semidiurnal band (~30° h^{-1}) spreads throughout the frequency range by non-linear interaction. A question arises as to the possibility that the 3.4 and 2.4 h edge waves are simply compound or overtides which are amplified by the bathymetry, after all, their frequencies correspond to S_7 and S_{10} tides, respectively. However, the S_2 tide on the Canterbury coast is almost negligible, varying from 10% of M_2 at Timaru to 5% of M_2 at Kaikoura (Goring & Bell 1995). A more likely source would be M_7 and M_{10} tides, corresponding to periods of 3.5 and 2.5 h respectively. However, inspection of Fig. 5 shows that even allowing for lack of precision in the results, the periodicity bands are centered on the 3.4 and 2.4 h periods. Therefore, the edge waves cannot be overtides of M_2. The possibility remains that they are compound tides (formed by combinations of M_2, N_2, and other minor tides), however, the high degree of variability of amplitude and phase of the edge waves seems to preclude the source being tidal. There needs to be some randomness in the forcing function to generate the variability shown in Fig. 6. The weather band (1–10° h^{-1} in Fig. 7) provides this. Therefore, we postulate that the main driving force is the non-linear interaction between semidiurnal tides and wind and barometric pressure changes to spawn higher harmonics. These higher harmonics are likely to be quite small and for a straight coastline may be dissipated by friction, but for the Canterbury coast they are amplified by the combined effect of the curved nature of the coastline and the bathymetry. Further research using numerical models is planned to investigate this hypothesis.

Another aspect which requires investigation is whether a tsunami could excite these edge waves, resulting in amplification and causing extensive damage on the Canterbury coastline. Indeed, preliminary modelling indicates that a wave of 3.4 h period along the eastern boundary of the model grid (Fig. 4) is amplified 100-fold at Sumner Head.

CONCLUSIONS

The oscillations observed on the peaks and troughs of sea level records from the Canterbury coast appear to be modelled correctly by a barotropic model and may be approximated by zero-mode edge waves. In the Canterbury Bight the edge waves have a predominant period of 2.4 h and appear to be trapped laterally by the curvature of the shoreline and Banks Peninsula. In Pegasus Bay they have a predominant 3.4 h period and appear to be trapped laterally between Banks Peninsula and the northern extent of the bay.

Numerical modelling indicates that rotation (Coriolis force) has only a minor effect on the waves and neglecting it does not alter the main results. This implies that an analytical model of the offshore shape of the waves (i.e., $F(x)$) may be possible using irrotational flow. Such a model would need to include a more realistic bathymetry than the semi-infinite sloping beach of Stokes or the sloping shelf of finite width described by LeBlond & Mysak (1978) in order to explain the sinusoidal shape of the function relative to its exponential decay.

The waves are highly variable in amplitude and phase and we postulate that they are generated by non-linear interaction between the semidiurnal tides and winds and barometric pressure changes. Further work is planned to investigate the source of the waves using both analytical and numerical modelling.

ACKNOWLEDGMENTS

We acknowledge the assistance of Glenn Carter of NIWA Christchurch in the preparation of the finite element grid and Roy Walters of USGS for his advice and assistance in the use of his TIDE2D model. We are grateful to the following organisations for their assistance in providing sea level data: Canterbury Regional Council, University of Canterbury Department of Geography, Lyttelton and Timaru Port Companies. Two anonymous reviewers contributed helpful comments and suggestions. This work was supported by the New Zealand Foundation for Research Science and Technology under Contract CO1422 and the National Tidal Facility (Adelaide).

REFERENCES

Abramowitz, M.; Stegun, I. A. 1964: Handbook of mathematical functions. New York, Dover.

Bendat, J. S. 1990: Nonlinear system analysis and identification from random data. New York, John Wiley & Sons.

Chiswell, S. M. 1994: Acoustic Doppler Profiler measurements over the Chatham Rise. *New Zealand Journal of marine and freshwater research 28*: 167–178.

Davies, A. M.; Jones, J. E.; Xing, J. 1997: Review of recent developments in tidal hydrodynamic modeling. I. Spectral models. *ASCE Journal of hydraulic engineering 123(4)*: 278–292.

Goring, D. G. 1984: Analysis of tidal river records by a harmonic regressive technique. *Journal of hydrology (Elsevier) 73*: 21–37.

Goring, D. G.; Bell, R. G. 1995: Variations of sea level on the Canterbury coast of New Zealand. *In*: Proceedings of the 12th Australasian Conference on Coastal and Ocean Engineering, Melbourne. Pp. 275–278.

Goring, D. G.; Bell, R. G. 1996: Distilling information from patchy tide gauge records: the New Zealand experience. *Marine geodesy 19*: 63–76.

Greig, M. J.; Gilmour, A. E. 1992: Flow through the Mernoo Saddle, New Zealand. *New Zealand journal of marine and freshwater research 26*: 155–165.

Heath, R. A. 1976: The response of several New Zealand harbours to the 1960 Chilean tsunami. In: Tsunami Research Symposium 1974. *Bulletin of the Royal Society of New Zealand 15*: 71–82.

Heath, R. A. 1979: Edge waves on the New Zealand east coast. *Marine geodesy 2(4)*: 337–350.

Heath, R. A. 1982: Generation of 2–3 hour oscillations on the east coast of New Zealand. *New Zealand journal of marine and freshwater research 16*: 111–117.

Heath, R. A. 1983: Observations on Chatham Rise currents. *New Zealand journal of marine and freshwater research 17*: 321–330.

Henry, R. F.; Walters, R. A. 1993: Geometrically based automatic generator for irregular triangular networks. *Numerical methods in engineering 9*: 555–566.

Himmelblau, D. M. 1970: Process analysis by statistical methods. New York, John Wiley & Sons.

LeBlond, P. H.; Mysak, L. A. 1978: Waves in the Ocean. Amsterdam, Elsevier Science Publishers B.V.

Lindstrom, J.; Kokko, H.; Ranta, E. 1997: Detecting periodicity in short and noisy time series data. *OIKOS 78(2)*: 406–410.

Marone, E.; de Mesquita, A. R. 1994: On nonlinear analysis of tidal records. *Continental shelf research 14(6)*: 577–588.

Otnes, R. K; Enochson, L. 1978: Applied time series analysis. John Wiley & Sons.

Pisarenko, V. F. 1972: On the estimation of spectra by means of non-linear functions of the covariance matrix. *Geophysical journal of the Royal Astronomical Society 28*: 511–531.

Walters, R. A. 1988: A finite element model for tides and currents with field applications. *Communications in applied numerical methods 4*: 401–411.